Complexes Between 1,1′-Binaphthyl-2,2′-Dicarboxylic Acid and Pyrazoles: A Case of Manual Sorting of Conglomerate Crystals (Triage)

by **Orm Hager**, **Antonio L. Llamas-Saiz**, and **Concepción Foces-Foces***

Departamento de Cristalografía, Instituto de Química-Física 'Rocasolano', CSIC, Serrano, 119,
E-28006 Madrid, Spain

Rosa M. Claramunt* and **Concepción López**

Departamento de Química Orgánica y Biología, Facultad de Ciencias, UNED, Senda del Rey, 9,
E-28040 Madrid, Spain

and **José Elguero**

Instituto de Química Médica, Centro de Química Orgánica Manuel Lora-Tamayo, CSIC, Juan de la Cierva, 3,
E-28006 Madrid, Spain

Dedicated to Professor *Jack D. Dunitz* on the occasion of his 76th birthday

The crystal and molecular structure of two salts, **I** and **III**, and one molecular complex, **II**, formed by combining 1,1′-binaphthyl-2,2′-dicarboxylic acid (BNDA) with pyrazole (**3**) and 3,5-dimethylpyrazole (**4**) has been determined by X-ray crystallography. The most striking feature is the spontaneous resolution of the racemic BNDA host by co-crystallization with **4**, an achiral guest, to form the salt **III**. The absolute configuration of three manually selected crystals of **III** have been established by crystallographic methods. The two crystals formed by the (*P*)-enantiomer display a negative *Cotton* effect. ^{13}C-CPMAS-NMR Spectroscopy has been used to compare the compounds obtained by crystallization with those prepared by mechanical grinding.

1. Introduction. – The manual sorting of a conglomerate is forever associated with *Louis Pasteur* [1][2]. This technique known as triage [3][4] is somewhat erratic, and few examples are well documented. To differentiate individual crystals of two enantiomers by inspection of their outward shape (generally under the microscope), the crystals must be hemihedral and possess hemihedral faces (hemihedry). The space groups $P2_1$ and $P2_12_12_1$ account for *ca.* 80% of chiral crystals; the probability of finding hemihedral faces is good in $P2_1$ and poor in $P2_12_12_1$ [4]. In this work, we will report a case of spontaneous resolution of a host induced by an achiral guest.

1,1′-Binaphthyl-2,2′-dicarboxylic acid (BNDA; **1**) belongs to a class of new hosts designed by *E. Weber* on rational bases [5]. These 'scissors-type' dicarboxylic acids yield a large number of crystalline compounds with different solvents. Its complexes with imidazole (**2**) have been used to model the active site of serine protease enzymes [6]. As many 2,2′-disubstituted 1,1′-binaphthalenes, BNDA (**1**) is racemic, and its methyl ester has been resolved [7]. The configuration of these compounds with axial chirality can be described indistinctly using the (*R*)/(*S*) or the (*P*)/(*M*) descriptors (the correspondence of (*R*) with (*M*), and (*S*) with (*P*) is general) [4].

Due to our interest in the H-bonds and intermolecular proton transfer shown, in the solid state, by *N*-unsubstituted pyrazoles, free [8–10] or as guests [11–13], we decided

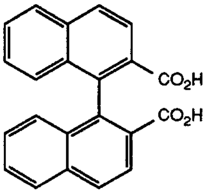

1 (±)-BNDA

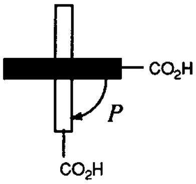

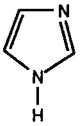

2

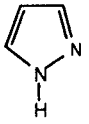

3

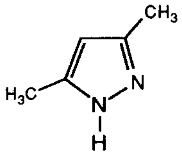

4

to study the interaction between **1** and pyrazole (**3**), and between **1** and 3,5-dimethylpyrazole (**4**).

2. Results and Discussion. – There are several possibilities for the formation of complexes between BNDA (**1**), and pyrazoles **3** and **4**. According to our results (see below), we have considered the following four cases (two salts, **I** and **III**, and two molecular complexes, **II** and **IV**).

Complex $\mathbf{1}+\mathbf{3}=\mathbf{I}$, $\mathrm{CO_2^-}\cdots\mathbf{3H}^+$
Complex $\mathbf{1}+[\mathbf{3}]_2=\mathbf{II}$, $\mathrm{CO_2H}\cdots\mathbf{3}\cdots\mathbf{3}$
Complex $\mathbf{1}+\mathbf{4}=\mathbf{III}$, $\mathrm{CO_2^-}\cdots\mathbf{4H}^+$
Complex $\mathbf{1}+[\mathbf{4}]_2=\mathbf{IV}$, $\mathrm{CO_2H}\cdots\mathbf{4}\cdots\mathbf{4}$

Complex **IV** is a hypothetical case that has been considered only for the discussion because of its analogy with complex **II** formed by **3**. However, the only structure we have obtained by combining **1** and **4** is **III**, independently of the stoichiometry used.

2.1. *X-Ray Crystal Structures.* The main geometrical parameters of the molecular structures for **I**, **II**, and **III** are given in *Table 1* using the numbering system displayed in *Fig. 1. Table 1* also contains the mean values (estimated standard deviation of the sample in parenthesis) of selected geometrical parameters of 13 structures of BNDA (**1**) complexes, one hydrated BNDA salt, and that of the pure host retrieved from the *Cambridge Structural Database* (CSD; October 1998 release [14]). The CSD reference codes with the name of the guest in parenthesis are: CILLUE (MeOH), CILMAL (EtOH), CILMEP (i-PrOH), CILMIT (i-BuOH), CILMOZ (ethylene glycol), CITRUS10 (imidazolium, $\mathbf{2H}^+$), CITSAZ10 (imidazole, **2**), CIWJEX10 (DMSO), CIWJIB10 (DMF), DOGXUS (PhBr), NATLUP (EtOH), TANDAN (*t*-BuOH), TITZEB (acetylacetone), VEVLOX (AcOH), and NATMAW the pure host. All these compounds are racemic structures including both BNDA (**1**) enantiomers in the crystal. The predominant host-guest ratio is 1:1 (7 complexes + 1 salt) followed by 1:2 (4 complexes), and finally the 2:1 and 2:3 stoichiometries with one example of each. In our case, complex **II** presents a 1:2 ratio that it is neither the most frequent, nor the one displayed by the related BNDA-imidazole complex ($\mathrm{CO_2H}\cdots\mathbf{2}$, CITSAZ10).

There are no significant differences in the molecular structures of the host moieties, as far as bond distances and angles are concerned, between **I**, **II** and **III** on one side, and with the previous structures reported on the other, excluding those related with the second carboxylic group in **II** (labelled using primes) when compared with the corresponding carboxylate groups in **I** and **III**. However, there are some differences in the torsion angles that are worth of mention. The most significant ($\sim 5\sigma$ compared with

Table 1. *Selected Geometrical Parameters for* **I**, **II**, *and* **III**, *and Mean Values of Neutral BNDA Moieties Retrieved from CSD* (Å,°). Duplicate values due to molecular symmetry are in italics

Compound	**I**	**II**		**III**	CSD
C(1)–C(1′)	1.499(2)	1.499(3)		1.507(4)	1.499(14)
C(1)–C(2)	1.382(3)	1.380(3)		1.381(5)	1.379(11)
C(2)–C(9)	1.493(2)	1.488(3)		1.491(4)	1.487(15)
C(9)–O(10)	1.213(2)	1.216(3)		1.207(3)	1.213(17)
C(9)–O(11)	1.323(2)	1.320(3)		1.318(4)	1.295(25)
C(1′)–C(2′)	1.376(2)	1.383(3)		1.386(5)	*1.379(11)*
C(2′)–C(9′)	1.501(2)	1.489(3)		1.501(4)	*1.487(15)*
C(9′)–O(10′)	1.254(2)	1.199(3)		1.260(4)	*1.213(17)*
C(9′)–O(11′)	1.242(2)	1.296(3)		1.255(5)	*1.295(25)*
N(1g)–N(2g)	1.342(2)	1.347(3)	1.336(3)	1.352(4)	
N(1g)–C(5g)	1.327(2)	1.336(3)	1.329(4)	1.337(4)	
N(1g)–H(1g)	0.96(3)	0.92(3)	0.92(3)	0.95(5)	
N(2g)–C(3g)	1.326(2)	1.325(4)	1.323(5)	1.330(4)	
N(2g)–H(2g)	0.96(3)	–	–	1.15(5)	
C(3g)–C(4g)	1.369(2)	1.388(4)	1.366(4)	1.385(5)	
C(4g)–C(5g)	1.371(3)	1.358(4)	1.365(5)	1.378(4)	
C(8a)–C(1)–C(1′)	117.9(1)	118.2(2)		118.3(2)	117.6(12)
C(2)–C(1)–C(1′)	123.0(1)	122.8(2)		123.0(3)	123.0(10)
C(2)–C(1)–C(8a)	119.1(1)	119.1(2)		118.7(3)	119.4(10)
C(1)–C(2)–C(9)	121.2(1)	120.3(2)		123.0(3)	
C(1)–C(2)–C(3)	120.5(1)	121.1(2)		120.7(3)	
C(3)–C(2)–C(9)	118.3(1)	118.6(2)		116.3(2)	
C(2)–C(9)–O(11)	112.3(1)	114.1(2)		112.1(2)	
C(2)–C(9)–O(10)	124.4(1)	124.0(2)		125.4(3)	
O(10)–C(9)–O(11)	123.3(2)	121.9(2)		122.5(3)	122.5(25)
C(1)–C(1′)–C(8a′)	119.4(1)	118.7(2)		118.8(2)	*117.6(12)*
C(1)–C(1′)–C(2′)	121.2(1)	121.6(2)		122.0(3)	*123.0(10)*
C(2′)–C(1′)–C(8a′)	119.3(1)	119.7(2)		119.2(3)	*119.4(10)*
C(1′)–C(2′)–C(9′)	121.7(1)	121.0(2)		123.5(3)	
C(1′)–C(2′)–C(3′)	120.9(1)	120.2(2)		119.9(3)	
C(3′)–C(2′)–C(9′)	117.4(1)	118.9(2)		116.6(3)	
C(2′)–C(9′)–O(11′)	119.0(1)	114.4(2)		119.3(3)	
C(2′)–C(9′)–O(10′)	119.5(1)	123.7(2)		119.5(3)	
O(10′)–C(9′)–O(11′)	121.5(2)	121.9(2)		121.1(3)	*122.5(25)*
N(2g)–N(1g)–C(5g)	108.1(2)	111.8(2)	111.0(2)	110.2(3)	
N(1g)–N(2g)–C(3g)	108.9(2)	104.3(2)	105.4(2)	107.6(3)	
N(2g)–C(3g)–C(4g)	108.6(2)	111.7(3)	111.3(3)	108.6(3)	
C(3g)–C(4g)–C(5g)	105.5(2)	104.6(2)	104.8(3)	106.7(3)	
N(1g)–C(5g)–C(4g)	109.0(2)	107.5(2)	107.6(3)	106.9(3)	
C(2)–C(1)–C(1′)–C(2′)	−86.3(2)	−87.7(3)		87.5(4)	94(6)
C(1′)–C(1)–C(8a)–C(8)	−1.3(2)	32.4(3)		−3.3(5)	
C(1′)–C(1)–C(2)–C(9)	−0.3(2)	−1.4(3)		3.4(5)	
C(1)–C(2)–C(9)–O(10)	−30.7(2)	−16.3(3)		26.1(5)	16(12)
C(1)–C(1′)–C(8a′)–C(8′)	−7.3(2)	2.7(3)		0.9(5)	
C(1)–C(1′)–C(2′)–C(9′)	3.0(2)	0.8(3)		0.4(5)	
C(1′)–C(2′)–C(9′)–O(10′)	75.9(2)	29.7(3)		12.8(5)	*16(12)*

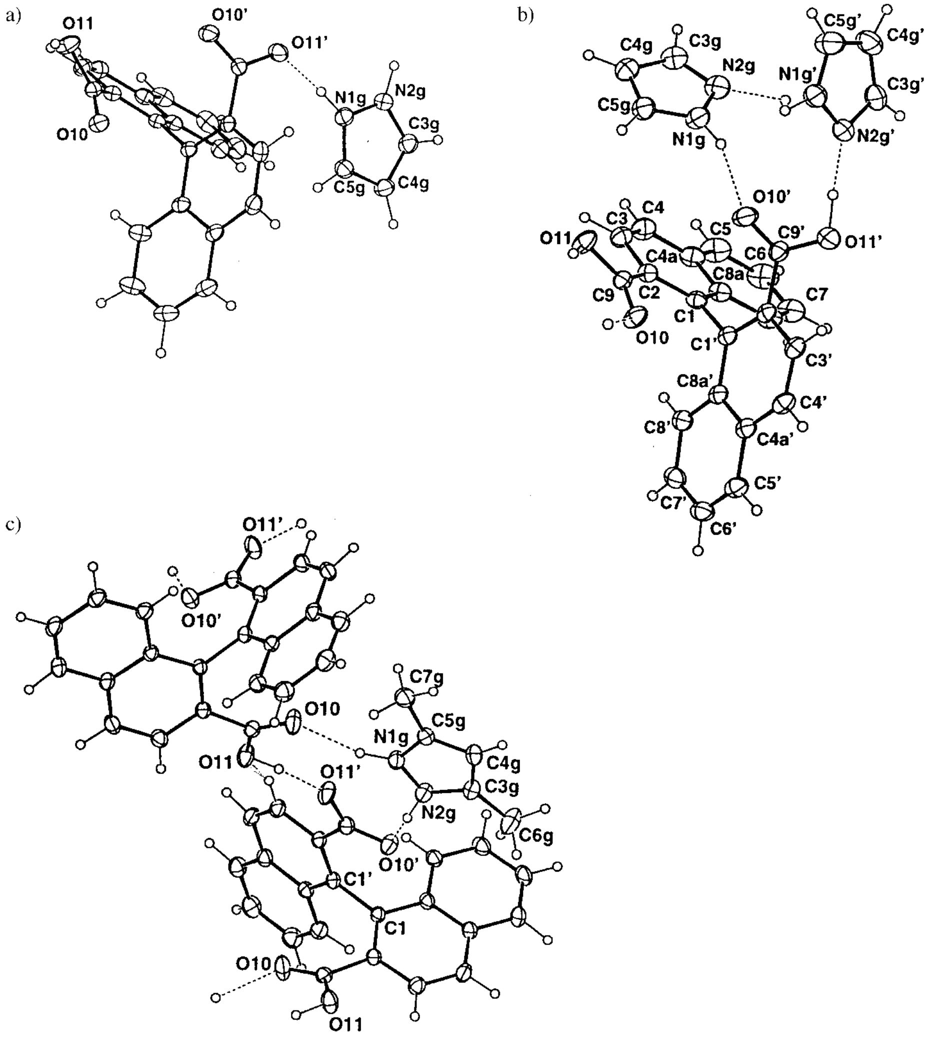

Fig. 1. *A perspective view of the crystallographically independent molecules of* **I** (a) *and* **II** (b) *showing the numbering system.* c) *Same as before for* **III** *plus one* 2_1*-axis related molecule of the host that has also been included to complete the cyclic* H-bond *arrangement.* Dotted lines indicate H-bonds. Displacement ellipsoids are drawn at 30% probability level.

the mean value obtained from the CSD) is that concerning the torsion of the carboxylate group in **I** that is further out of the naphthalene plane. The C–C–C–O torsion angle (75.9(2)°) is clearly out of the range (0–53°) displayed by other structures. Although not statistically significant, the torsion angle between both naphthalene moieties in the three structures reported here is smaller and close to the lower limit of the above mentioned 13 structures found in the CSD [87.4–108.0°].

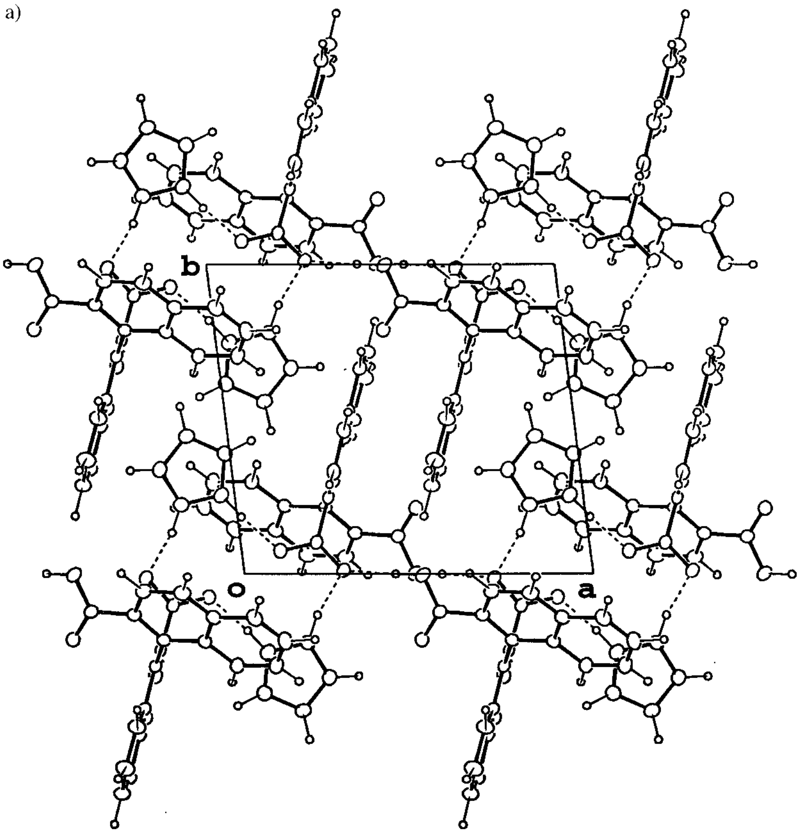

Fig. 2. a) *Packing diagram of* **I** *down the* c *axis.* Dotted lines indicate H-bonds. Displacement ellipsoids are drawn at 30% probability level.

There are clear differences in the molecular structures of the pyrazole guests (*Table 1*), mainly in the bond angles, which clearly show the presence of pyrazole in **II** (more asymmetric geometry) and pyrazolium cations in **I** and **III** (more symmetric geometry), although, in **III**, the bond angles at the N-atoms are significantly different due to the very strong and asymmetric pattern of the H-bonds (*Table 2*). In all cases, the position of the H-atoms has been unambiguously determined in the *Fourier* difference synthesis (see *Exper. Part*). Only in the second molecule of **II** (labelled with primes) and in **III**, the heterocyclic rings do deviate significantly from planarity (χ^2 values of 11.93, 8.55, 2.08, and 3.23, resp., *vs.* a tabulated value of 5.99 at 95% probability level).

The crystal packing is different in all complexes. The secondary structure is formed by conventional H-bonds where the donor and acceptor groups are either neutral or charged N- or O-atoms (*Figs. 2*, *3*, and *4*), while the tertiary structure is made up by weaker H-interactions of C–H$\cdots$O/N/π types (*Table 2*). The secondary structure of **I**–**III** can be described in more detail as follows:

In **I**, a $N_2:R_4^4(14)$ [15] centrosymmetric dimer (BNDA$^-$ **3**H^+)$_2$ is formed *via* N^+–H $\cdots O^-$ H-bonds. These subunits are joined in chains along the crystallographic *a* axis by

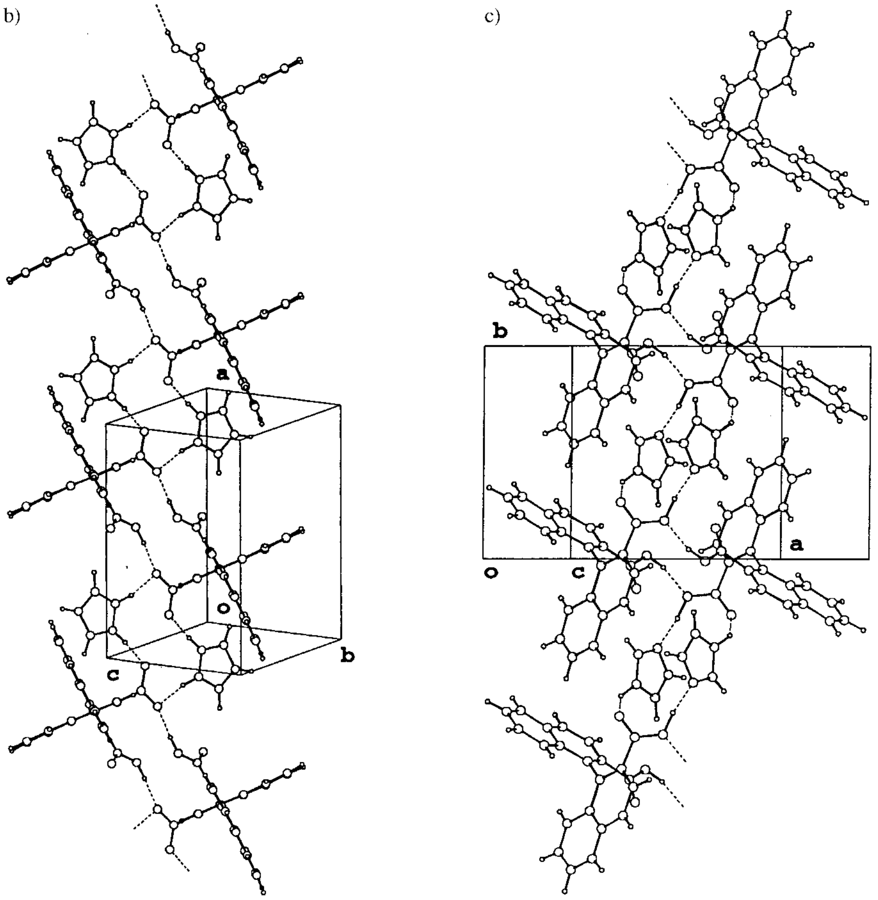

Fig. 2. b) *Perpendicular view of one chain of H-bonded molecules in* **I**. c) *Same as* b) *for CITSAZ10.*

means of another cyclic and centrosymmetric pattern of H-bonds, $N_1:R_2^2(18)$, formed between the carboxylic OH groups and one carboxylate O-atom (*Fig. 2,a*). This secondary structure, $N_3:C_3^3(14)\ [R_2^2(18)R_4^4(14)]$, formed by chains of molecules, is topologically similar to that present in the 1:1 complex BNDA-imidazole (**2**; CSD Refcode: CITSAZ10), $N_3:C_3^3(15)[R_2^2(18)R_4^4(16)]$ (*Fig. 2,b* and *c*), assuming that, in this case, the acid proton has been transferred to the guest molecule. The small differences in the degree of some graph sets are due to the presence of a C-atom between the N-atoms in imidazole compared with pyrazole.

In **II**, one carboxylic group is involved, together with both crystallographically independent pyrazole guest molecules, in infinite chains of H-bonds along the crystallographic 2_1 symmetry axes ($N_3:C_3^3(10)$). The other carboxylic group forms, with its centrosymmetrically related counterpart, the usual carboxylic-acid H-bonded dimer [16] ($N_1:R_2^2(8)$) joining the previously described chains in a kind of *zig-zag* sheet which extends in the *bc* plane (*Fig. 3*).

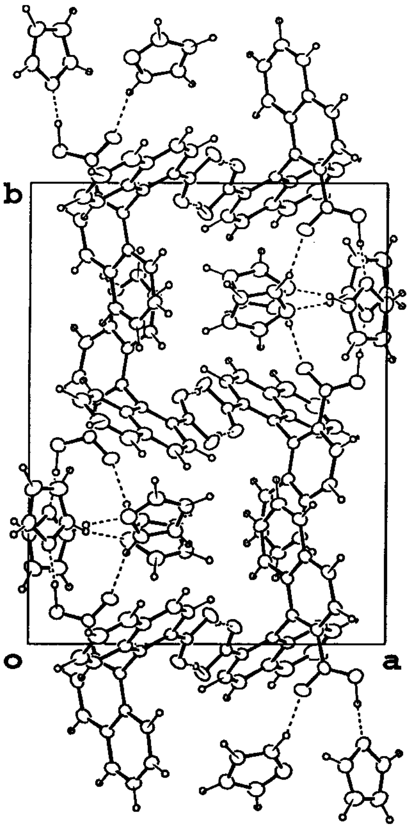

Fig. 3. *Packing diagram of* **II** *down the* c *axis*

Finally, in **III**, the molecules (two 2_1-symmetry-related BNDA anions and the pyrazolium cation **4H**$^+$) are linked through H-bonds in a cyclic motif (N_3:$R_3^3(11)$), leading to the formation of N_1:C(9), N_2:$C_2^2(12)$ chains along the 2_1 symmetry axes (*Fig. 4,a* and *b*). Chains of molecules with very similar topologies (N_1:C(9), N_2:$C_2^2(11)$), again including a N_3:$R_3^3(10)$ cyclic motif, are displayed by the BNDA-(*t*-BuOH) complex (TANDAN) formed by molecules related by the monoclinic 2_1 symmetry axes (*Fig. 4,c*). In this structure, each chain is accompanied by its centrosymmetrically related counterpart to give rise to the whole crystal. However, in **III** all chains display the same absolute configuration, and, therefore, each single crystal is formed by molecules of only one BNDA enantiomer. In both cases, TANDAN and **III**, there are three C–H···O interactions linking different H-bonded chains of molecules (*Table 2*). While in **III** all interactions occur between chains related by a crystallographic translation, in TANDAN two of them occur between centrosymmetrically related chains, each formed by one enantiomer, and only one interaction links chains related by a 2_1 axis (formed by the same enantiomer). It has been determined with the program HOLES [17] and the *van der Waals* radii reported in [18] that there are no voids left in any of the crystal structures. The total packing coefficients obtained

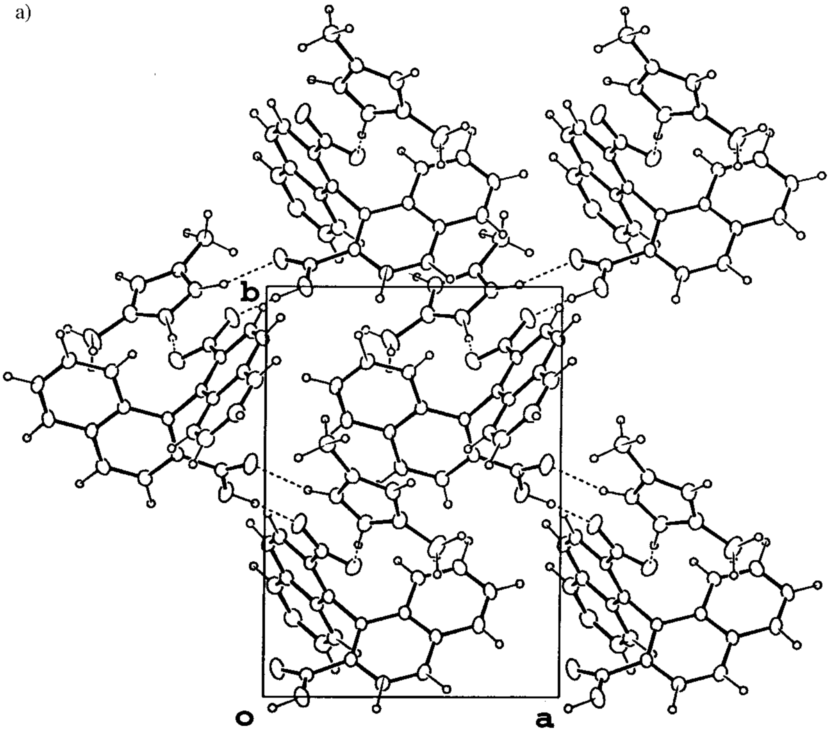

Fig. 4. a) *Packing diagram of* **III** *down the* c *axis.*

by this procedure are 0.700, 0.670, and 0.687 for **I**, **II**, and **III**, respectively. The largest values correspond to the two salts, more closely packed, although there is a small difference between them indicating the better packing in the racemic structure, **I**, compared with the resolved one, **III**.

2.2. *^{13}C-CPMAS-NMR Spectroscopy.* We have collected in *Table 3* all the ^{13}C chemical shifts necessary for the discussion: compounds **1**, **3**, and **4** in neutral solution, compounds **3** and **4** in acid solution (cations **3H**$^+$ and **4H**$^+$), solid-state ^{13}C-CPMAS results of compounds **1**, **3**, **4**, **3H**$^+$, and **4H**$^+$, crystals of the complexes **I**, **II**, and **III**, mechanical mixtures (co-grinding) of **1** + **3** (1 : 1), **1** + **3** (1 : 2), **1** + **4** (1 : 1), **1** + **4** (1 : 2). Due to lack of information from the literature, the ^{1}H- (8.12 (H–C(3)), 8.09 (H–C(4), 8.04 (H–C(5)), 7.54 (H–C(6)), 7.27 (H–C(7)), 6.91 (H–C(8)); J(3,4) = 8.7, J(5,6) = 8.0, J(5,7) = 1.3, J(6,7) = 6.8, J(6,8) = 1.1, J(7,8) = 8.3) and ^{13}C-NMR spectra, chemical shifts, and ^{1}H,^{13}C coupling constants of BNDA (**1**) in (D_6) DMSO solution were assigned using COSY (^{1}H,^{1}H), HMQC, and HMBC experi ments.

We have summarized below a highly simplified version of the most relevant information we obtained (solution and solid state) concerning BNDA (**1**) and pyrazoles **3** and **4**. The most differential signals between neutral and monoanionic BNDA are those corresponding to the C-atoms C=O, C(1), and C(2).

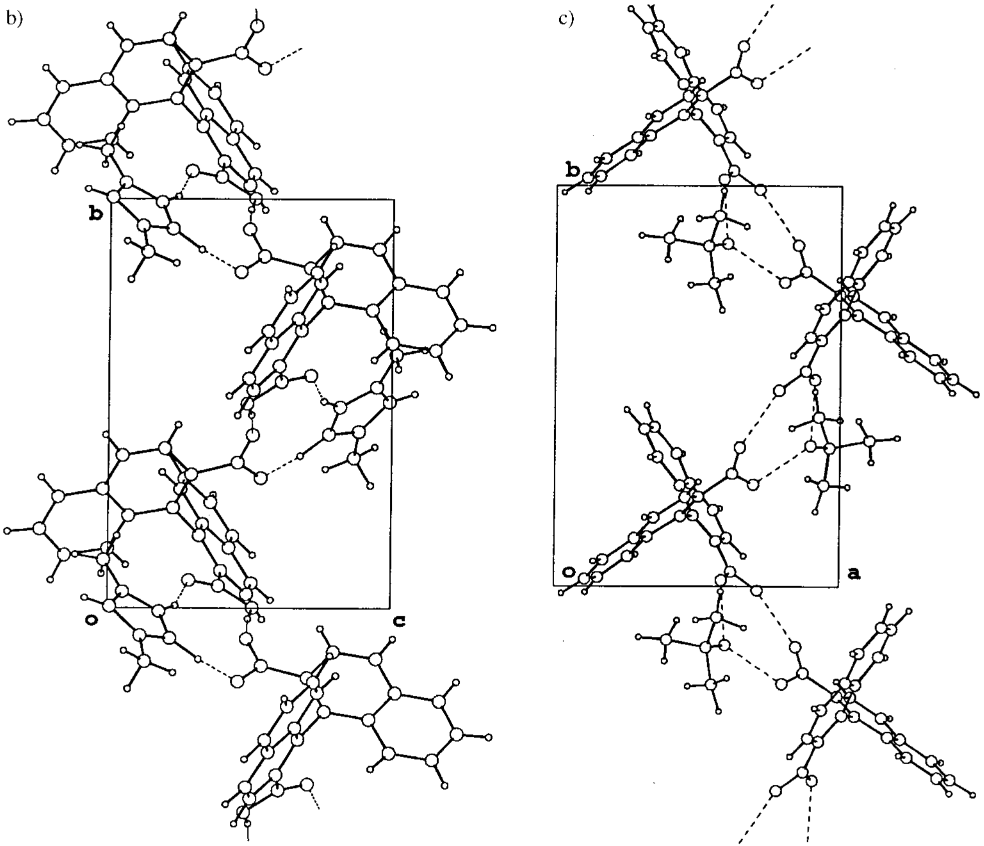

Fig. 4. b) *View of one chain of H-bonded molecules in* **III** *along the* a *axis.* c) *Similar chain of molecules in TANDAN down the* c *axis.* The H-atoms involved in the cyclic pattern of H-bonds have been omitted because of their dubious positions due to the reported apparent disorder of the guest molecule (*t*-BuOH).

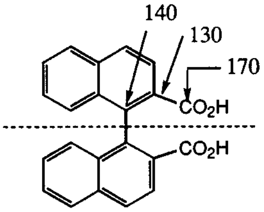

1

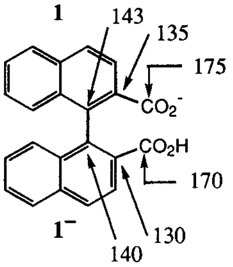

1⁻

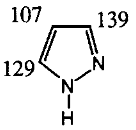

3

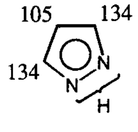

3

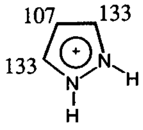

3H⁺

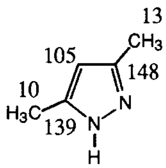

4

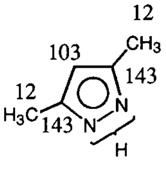

4

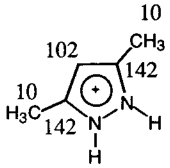

4H⁺

Table 2. *Selected H-Interactions for Compounds* **I**, **II**, *and* ***III*** (Å,°)

	D–H	HA	D···A	D–H···A
Compound **I**				
O(11)–H(11)···O(10′) $(1-x,-y,1-z)$	0.94(3)	1.73(3)	2.658(2)	172(3)
N(1g)–H(1g)···O(11′)	0.96(3)	1.66(3)	2.623(2)	174(3)
N(2g)–H(2g)···O(10′) $(-x,-y,1-z)$	0.96(2)	1.72(2)	2.666(2)	168(3)
C(3g)–H(3g)···O(10) $(x-1,y,z)$	0.96(3)	2.38(3)	3.260(2)	153(2)
C(4)–H(4)···O(11′) $(x,y,z-1)$	0.99(3)	2.82(2)	3.599(2)	136(2)
C(5)–H(5)···O(11′) $(-x,-y,-z)$	0.98(3)	2.62(3)	3.602(2)	174(2)
C(5′)–H(5′)···O(10) $(1-x,1-y,1-z)$	0.98(3)	2.64(3)	3.568(3)	159(2)
C(6′)–H(6′)···O(11) $(x,y+1,z)$	1.02(3)	2.67(3)	3.379(2)	127(2)
C(7′)–H(7′)···O(10) $(1-x,1-y,-z)$	0.99(3)	2.63(3)	3.611(2)	172(2)
C(4g)–H(4g)···Cent(2) $(-x,1-y,-z)$a)	0.96(3)	2.95(2)	3.700(2)	136(2)
C(5g)–H(5g)···Cent(1′)a)	0.97(2)	2.95(3)	3.785(2)	146(2)
Compound **II**				
O(11)–H(11)···O(10) $(1-x,1-y,1-z)$	0.95(5)	1.72(5)	2.656(2)	168(5)
O(11′)–H(11′)···N(2g′)	1.05(4)	1.56(4)	2.604(3)	176(4)
N(1g′)–H(1g′)···N(2g) $(x,3/2-y,1/2+z)$	0.92(3)	1.91(3)	2.817(3)	167(3)
N(1g)–H(1g)···O(10′)	0.92(3)	1.98(3)	2.861(3)	158(3)
C(3g)–H(3g)···O(10′) $(x,3/2-y,z-1/2)$	1.00(3)	2.55(3)	3.374(3)	139(2)
C(3g)–H(3g)···O(11) $(x,3/2-y,z-1/2)$	1.00(3)	2.93(3)	3.632(3)	128(2)
C(4g)–H(4g)···O(10) $(1-x,y+1/2,1/2-z)$	0.99(3)	2.71(3)	3.448(3)	132(2)
C(5g)–H(5g)···O(11)	1.01(3)	2.89(3)	3.731(3)	141(2)
C(3′)–H(3′)···O(11′) $(2-x,1-y,1-z)$	0.97(3)	2.72(3)	3.562(3)	146(2)
C(5)–H(5)···N(2g) $(x,3/2-y,z-1/2)$	0.99(3)	2.86(3)	3.657(3)	139(2)
C(4′)–H(4′)···N(2g′) $(2-x,1-y,1-z)$	0.95(3)	2.83(3)	3.645(3)	144(2)
C(5)–H(5)···Cent(1g) $(x,3/2-y,z-1/2)$a)	0.99(3)	2.71(3)	3.616(3)	154(2)
C(5g′)–H(5g′)···Cent(2) $(x,3/2-y,1/2+z)$a)	0.97(4)	2.77(4)	3.483(3)	131(3)
C(4g′)–H(4g′)···Cent(1′) $(2-x,1/2+y,1/2-z)$a)	0.98(4)	2.99(3)	3.667(3)	127(2)
Compound ***III***b)				
N(2g)–H(2g)···O(10′)	1.15(5)	1.40(5)	2.544(4)	174(5)
O(11)–H(11)···O(11′) $(-x,y-1/2,1-z)$	0.98(5)	1.54(5)	2.516(3)	178(5)
N(1g)–H(1g)···O(10) $(-x,y+1/2,1-z)$	0.95(5)	2.01(5)	2.903(4)	155(4)
C(3′)–H(3′)···O(11) $(-x,y+1/2,1-z)$	0.96(–)	2.84(–)	3.659(4)	143(–)
C(5)–H(5)···O(11′) $(1-x,y-1/2,1-z)$	1.02(–)	2.82(–)	3.583(5)	132(–)
C(6′)–H(6′)···O(11) $(x,y,z-1)$	1.00(–)	2.75(–)	3.390(4)	122(–)
C(7′)–H(7′)···O(11) $(x,y,z-1)$	1.06(–)	2.70(–)	3.406(4)	124(–)

a) Cent(1′), Cent(2) and Cent(1g) stand for the centroids of the [C(1′), C(2′),...C(8a′)], [C(4a), C(5),... C(8a)], and [N(1),N(2),...C(5)] rings, respectively.

b) The last three CH···O interactions occur between different chains of H-bonded molecules (see text). The interchain interactions in TANDAN, using the same numbering scheme for BNDA, are: C(6)–H(6)···O(11) $(1/2-x,y-1/2,1/2-z)$ 1.01, 2.68, 3.667 Å, 166°; C(8)–H(8)···O(11′) $(1-x,-y,-z)$ 1.00, 2.77, 3.668 Å, 150°, and C(4)–H(4)···O(5g) $(1-x,-y,-z)$ 0.98, 2.96, 3.582 Å, 123°.

In the case of pyrazoles, two cases can be found for neutral molecules: without annular tautomerism (C(3) and C(5), Me(3) and Me(5) different) and average signals due to annular tautomerism (C(3) and C(5), Me(3) and Me(5) identical). In the case of pyrazole (**3**), different signals are observed in the solid state and average signals in solution. In the case of 3,5-dimethylpyrazole (**4**), average signals are observed both in solution and in the solid state at room temperature; to observe different signals for **4**, the ^{13}C-CPMAS spectrum should be recorded at low temperatures (*i.e.*, at −100°)

Table 3. *^{13}C-NMR Data for Compounds* **1**, **3**, **4**, **3 H$^+$**, **4 H$^+$**, **I**, **II**, *and* **III**

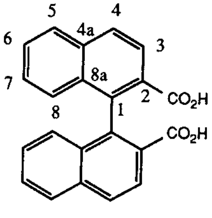

1 BNDA

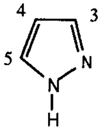

3

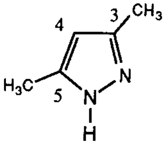

4

Compounds	Conditions	C(1)	C(2)	C(3)	C(4)	C(4a)	C(5)	C(6)	C(7)	C(8)	C(8a)	CO_2H	C(3)	C(4)	C(5)	Me(3)	Me(5)
1	a)b)	139.6	128.2	126.2	127.6	134.4	128.0	127.5	126.7	126.7	132.6	167.7	–	–	–	–	–
1	c)d)	139.6	129.5	125.6	128.0	134.7	129.5	128.0	125.6	125.6	132.8	170.1	–	–	–	–	–
3	b)	–	–	–	–	–	–	–	–	–	–	–	133.7	104.8	133.7	–	–
3	c)	–	–	–	–	–	–	–	–	–	–	–	138.7	107.0	128.8	–	–
4	b)	–	–	–	–	–	–	–	–	–	–	–	142.9	103.3	142.9	11.9	11.9
4	c)	–	–	–	–	–	–	–	–	–	–	–	147.5	104.8	139.3	12.8	10.5
3 H$^+$	e)	–	–	–	–	–	–	–	–	–	–	–	133.8	107.7	133.8	–	–
3 H$^+$	c)f)	–	–	–	–	–	–	–	–	–	–	–	133.3	107.0	133.3	–	–
4 H$^+$	e)	–	–	–	–	–	–	–	–	–	–	–	146.5	106.8	146.5	9.2	9.2
4 H$^+$	c)f)	–	–	–	–	–	–	–	–	–	–	–	145.8	105.5	145.8	10.2	10.2
I	c)	143.7 141.5	134.9 128.2	126.2	128.2	134.9	128.2	126.2	126.2	126.2	134.9	174.0 168.8	132.7	106.9	132.7	–	–
1 + **3** (1:1)g)	c)	143.0	132.0	125.2	127.3	135.2	127.3	125.2	125.2	125.2	133.0	173.3	135.2	104.4	129.4	–	–
II	c)	137.0	130.6	122.5	127.6	134.0	127.6	127.6	124.1	126.1	132.7	170.1 170.2	137.0	105.2	127.6	–	–
1 + **3** (1:2)g)	c)	141.0	130.5	127.0	127.0	133.1	127.0	127.0	127.0	127.0	133.1	170.2	137.0	104.2	127.0	–	–
III	c)	142.0 142.0	133.9 129.2	126.0	129.2	133.9	127.2	127.2	127.2	127.2	133.9	173.6 171.1	141.5	101.9	141.5	10.2	10.2
1 + **4** (1:1)g)	c)	143.0 141.6	135.6	126.0	127.3	135.6	127.8	127.8	126.0	126.0	133.7	173.7 171.2	141.6	101.9	141.6	10.2	10.2
1 + **4** (1:2)g)	c)	h)											143.0	104.9	143.0	11.5	11.5

---

a) Coupling-constant values in Hz are: C(1), $^3J = {^3J} = 4.2$; C(2), $^3J = 7.5$; C(3), $^1J = 163.7$; C(4), $^1J = 162.8$; C(4a), $^3J = {^3J} = {^3J} = 5.8$; C(5), $^1J = 160.5$; C(6), $^1J = 160.6$; C(7), $^1J = 160.0$, $^3J = 7.5$; C(8), $^1J = 160.0$, $^3J = 7.5$; C(8a), $^3J = {^3J} = {^3J} = 6.3$, CO_2H, $^2J = 2.8$. b) (D_6)DMSO. c) CPMAS. d) Contains EtOH as a guest (15.4 and 57.2 ppm). e) SO_4H_2. f) Trifluoroacetate salt. g) Mechanical co-grinding. h) This complex is a physical mixture (**III** + **4**), only the average signals corresponding to the excess of 3,5-dimethylpyrazole (**4**) are given.

[8][9][19]. Note that the average chemical shifts of the pyrazolium cations are not very different from those of the neutral pyrazoles [20].

The data reported in *Table 3* clearly show that complex **I** is a salt, **1**$^-$**3 H**$^+$, complex **II** is a neutral **1** + [**3**]$_2$ inclusion compound, the two neutral pyrazoles being magnetically equivalent and the NH proton localized (no proton transfer), finally complex **III** is a salt, **1**$^-$**4 H**$^+$.

2.3. *The Acid-Base Equilibrium*. The difference between salts **I** and **III**, and complex **II** is similar to the formation of salts **VI** and molecular complexes **V** in the case of benzoic acids **5** and pyridines **6**. Depending on the substituents R and R′, structures **V** or **VI** are observed (both in solution and in solid state) [21–23].

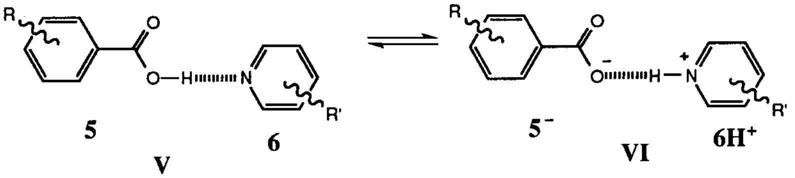

The displacement of a proton along the H-bond transforms a neutral complex into a salt: A–H···B → A$^-$···H–B$^+$. This elemental reaction almost never occurs in the gas phase (the BrH···NMe$_3$ complex is a possible exception) [24][25], a polar solvent being usually necessary. The crystal could play the role of the polar solvent with the advantage that the positions of all the heavy atoms are well defined. For this reason, there has been much interest in studying these proton transfers in the solid state. The prevailing point of view is that it is possible to find all the intermediate situations between A–H···B and A$^-$···H–B$^+$, such as [A···H···B]$^+$ [26][27].

It has been reported that host-guest compounds of defined structure can be prepared without the assistance of a solvent simply by mechanically co-grinding two components in a defined stoichiometry [28][29]. Even if no solvent was added, atmospheric water can be incorporated in the mixture, particularly with compounds so prone to form H-bonds, as carboxylic acids and pyrazoles.

We carried out a series of experiments (*Table 3*) and monitored them by ^{13}C-CPMAS NMR. The mixture obtained in the co-grinding experiment starting from **1** and **3** (1:1) is an inclusion compound; it is not a physical mixture of **1** and **3**, because there is a splitting of the C=O signal of BNDA (**1**), and it is not a salt like **I**, because the chemical shifts of the pyrazole correspond to a neutral molecule without annular tautomerism. When this complex is dissolved in AcOEt, and the solution is slowly evaporated, crystals of **I** are obtained. The mixture obtained co-grinding **1** and **3** (1:2) is identical to that obtained by crystallization; therefore, it has the **II** structure. The mixture corresponding to **1** + **4** (1:1) gives a ^{13}C-CPMAS-NMR spectrum practically identical to that of **III**; therefore, it is the same salt (**1**$^-$ **4 H**$^+$). Finally, complex **IV** (**1** + [**4**]$_2$) was ever obtained neither by crystallization neither by co-grinding. The ^{13}C-CPMAS-NMR spectrum corresponds to a physical mixture of **III** plus the average signals corresponding to the excess of 3,5-dimethylpyrazole (**4**) with rapid proton transfer (annular tautomerism).

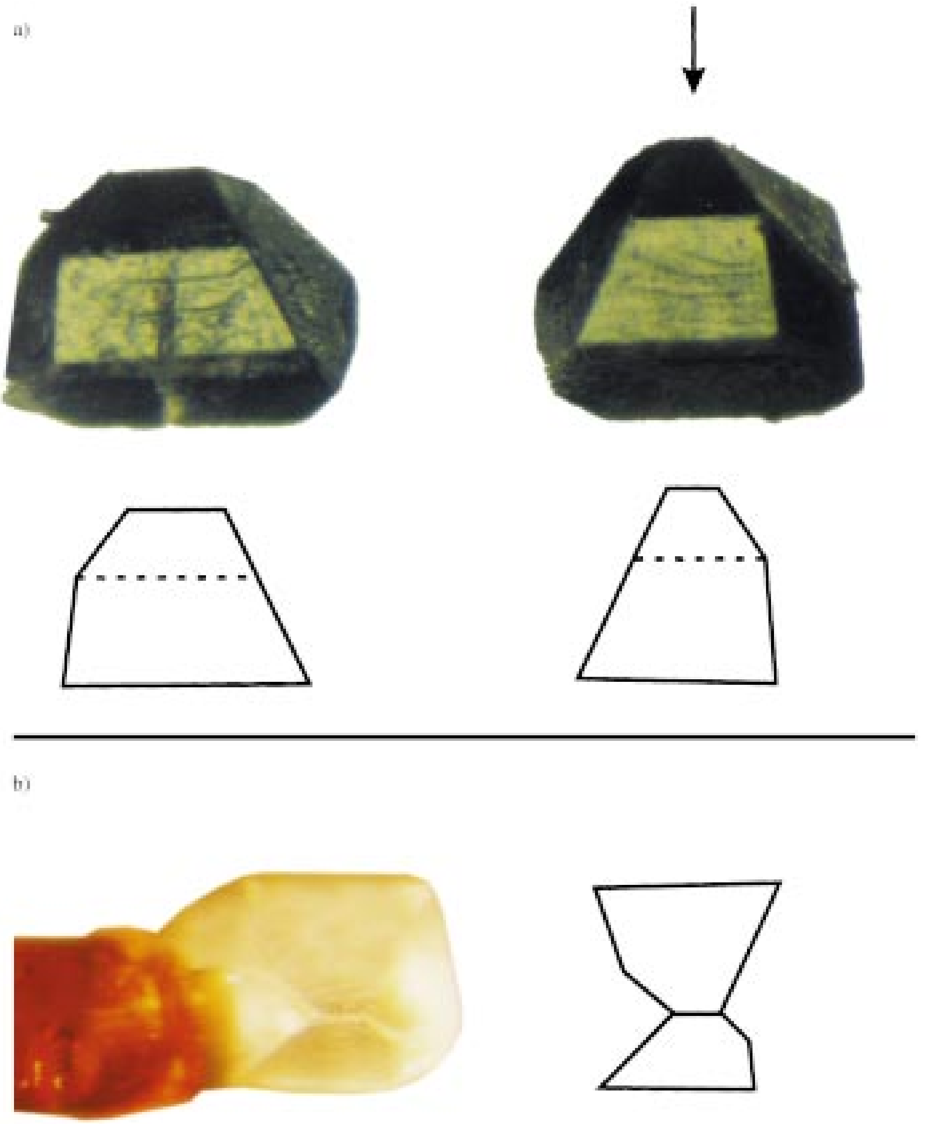

Fig. 5. a) *A photography of a pair of hemihedral crystals of salt* **III**. For clarity, one hemihedral face has been drawn below for each crystal; the dashed line represents a hidden edge of the crystal. The arrow indicates the viewpoint employed in *b* for crystal A used in the X-ray data collection. b) *View of the crystal A approximately along the* 2_1 *symmetry axis.* A pair of symmetry-related hemihedral faces is shown on the right.

The fact that 3,5-dimethylpyrazole (**4**) (pK_a = 4.06) is more basic than pyrazole (**3**) (pK_a = 2.48) [30] accounts for the different behavior of these two compounds towards BNDA (**1**), which is also consistent with the formation of the salt CITRUS10 [6] between BNDA (**1**) and imidazole (**2**) (pK_a = 6.99) [30]. There is also the neutral

BNDA/imidazole complex CITSAZ10, but the position of the H-atoms along the $CO_2H \cdots N(Im)$ is not clear, even the neutral structure of the complex being only tentative [30].

2.4. *Resolution of BNDA* (**1**). The triage of crystals of salt **III** was carried out under a microscope which precludes any preparative possibility. A series of five pairs of hemihedral crystals were selected (*Fig. 5,a*), five having the same habit (T1) as that used for the crystal structure determination (*Fig. 5,b*) and five others being enantiomorphs (T2). There were no errors in the triage: the CD spectra (see *Fig. 6*) and sign of the angle of rotation were in all cases consistent, those corresponding to the X-ray structure (crystal A) having a negative *Cotton* effect and an $[\alpha]_D^{25} = -100 \pm 5°$ (the large imprecision is due to the low solubility of the compound).

Conclusion. – This work has shown how two simple components, a benzoic acid derivative, BNDA (**1**), and pyrazoles, are able to yield a variety of interesting situations. The part concerning acid-base 'equilibria' in the solid state can be rationalized on simple grounds (H-bonds, pK_a values), thus providing a predictive model (*e.g.*, 4-nitroimidazoles, $pK_a = 0.05 - 0.86$ [29] should give inclusion compounds, not salts). The part concerning the spontaneous resolution of BNDA (**1**) is still beyond explanation.

All structures retrieved from CSD correspond to racemic BNDA, thus, up to now, only 3,5-dimethylpyrazole (**4**) is able to induce the spontaneous resolution of BNDA. The ability of **4** to act as a guest, to induce the crystallization of BNDA as a conglomerate and not, like all other hosts, as a racemic compound is not related to its facility to form chiral chains of 2_1 symmetry, because they are also formed by the *t*-BuOH guest (TANDAN). The difference between both cases is that in the first one, **III**, only chains of the same chirality are packed to form the crystals. This packing is achieved by means of weak intermolecular interactions, and among those, that of $C-H \cdots O$ type are the strongest ones, indicating the relevance of this kind of weak H-bonds in the chiral recognition phenomena.

In summary, the formation of **III** constitutes a new unusual case of spontaneous resolution of a racemic compound by co-crystallization with an achiral guest [31].

Spanish *DGICYT* (Project No. PB96-0001-C03) and the *European Community* (Project CHRXCT94-0582 and *NATO* grant CRG 971079) are greatly acknowledged for financial support. *O. H.* thanks project CHRXCT94-0582 for a grant. Our gratitude to Prof. *E. Weber* (Freiberg) for providing us with a generous amount of racemic BNDA, Prof. *Ch. Roussel* (Marseille) for useful comments concerning chiral resolution, and Drs. *N. Jagerovic* and *J. M. Andreu* (Madrid) for their help with the CD measurements.

Experimental Part

Preparation of Host **1**. Synthesis of racemic BNDA is given in [32].

Preparation of the Crystals Used in Structure Determination. Salts **I** *and* **III**. Although these salts corresponds to a 1:1 stoichiometry, a twofold excess of pyrazole was used. A soln. of 0.0092 g (0.027 mmol) of BNDA (**1**) in 1.5 ml of dry AcOEt was carefully covered with a soln. of the respective pyrazole (0.055 mmol in each case) in 1.5 ml AcOEt with a small amount of H_2O (*ca.* 5 μl). In a narrow test tube, this resulted in a two phase system and, at the intersection, well formed crystals grew in few hours. To obtain better-quality crystals, they were ground and recrystallized from dry EtOH/dry AcOEt 1:1. This procedure yielded the well formed crystals suitable for optical separation and for X-ray crystallography.

Complex **II** (*Inclusion Compound*). The same stoichiometry (1:2) was used. The previous method was modified, omitting the addition of H_2O and using a syringe to let the pyrazole soln. slowly flow into the BNDA

Table 4. *Crystal Analysis Parameters for Compounds* **I**, **II** *and* **III**

Crystal data	**I**	**II**	**III**
Formula	$C_{22}H_{13}O_4^- \cdot C_3H_5N_2^+$	$C_{22}H_{14}O_4 \cdot 2\,C_3H_4N_2$	$C_{22}H_{13}O_4^- \cdot C_5H_9N_2^+$
Crystal habit	Colorless, prism	Colorless, prism	Colorless, prism
Crystal size [mm]	0.33 × 0.26 × 0.20	0.40 × 0.30 × 0.30	0.43 × 0.33 × 0.23
Symmetry	Triclinic, *P*-1	Monoclinic, $P2_1/c$	Monoclinic, $P2_1$
Unit cell determination	Least-squares fit [33] from 81, 86, and 88 reflections ($\theta < 45°$)		
Unit cell dimensions [Å, °]:	$a = 11.8011(6)$	$a = 13.6549(7)$	$a = 9.5339(4)$
	$b = 10.3564(5)$	$b = 17.5532(14)$	$b = 12.8802(9)$
	$c = 8.8594(4)$	$c = 10.0218(4)$	$c = 9.0053(4)$
	$\alpha = 74.108(4)$	$\alpha = 90$	$\alpha = 90$
	$\beta = 108.712(3)$	$\beta = 90.061(3)$	$\beta = 100.525(3)$
	$\gamma = 101.944(5)$	$\gamma = 90$	$\gamma = 90$
Packing: *V* [Å^3], *Z*	977.9(1), 2	2402.1(2), 4	1087.2(1), 2
D_c[g/cm^3], *M*, *F*(000)	1.394, 410.43, 428	1.323, 478.51, 1000	1.339, 438.48, 460
μ [cm^{-1}]	7.816	7.393	7.365
T [K]	200	200	200
Experimental data			
Technique	Four circle diffractometer: *Philips PW1100* [34], Bisecting geometry. Graphite-oriented monochromator: $\omega/2\theta$ scans. Detector apertures 1 × 1°. 1 min./reflex. CuK_α radiation.		
Scan width	1.5°	1.6°	1.6°
$\theta_{\max}$	65°	65°	65°
Number of reflections:			
Measured	3409	4411	4154
Independent	3279	4018	1943 (*Friedel* pairs)
Observed ($2\sigma(I)$)	2989	3247	1925 (*Friedel* pairs)
Standard reflections:		2 reflexions every 90 min. No decay.	
Secondary extint. (× 10^4) [35]:	0.232(12)	0.221(10)	0.569(56)
Solution and refinement			
Solution		Direct methods: Sir92 [36]	
Refinement		Least-squares on F_{obs}, Full matrix	
Parameters			
Number of variables	352	413	311[a])
Degrees of freedom	2637	2834	1614
Ratio of freedom	8.5	7.9	6.2
Abs. struct. parameter [37]	–	–	0.19(30)
H-Atoms:		From difference synthesis	
Weighting scheme:	Empirical as to give no trends in $\langle w\Delta^2F\rangle$ *vs.* $\langle\,|F_{\text{obs}}|\,\rangle$ and $\langle\sin\theta/\lambda\rangle$		
Max. thermal value [Å^2]	U_{33}[O(11′)] = 0.077(8)	U_{33}[O(10′) = 0.126(2)	U_{22}[C(6g)] = 0.082(3)
Final ΔF peaks [eÅ^{-3}]	−0.24/0.19	−0.39/0.39	−0.16/0.19
Final R and R_w	0.037, 0.044	0.049, 0.056	0.037, 0.044

[a]) All H-atoms bonded to C-atoms have been kept fixed in the refinement.

soln. The mass of crystals took about two weeks to grow, which was freed from the pyrazole in excess by rinsing it with AcOEt (complex **II** is dissolved in AcOEt extremely slowly). In the case of **II**, crystals suitable for X-ray crystallography could be thus obtained; but in the case of **IV** (**1** + [**4**]$_2$) no compound with this composition can be obtained.

Crystallographic Data Collection and Structure Determination of **I**, **II**, *and* **III**. The most relevant details of data collection and those of the refinement procedure are given in *Table 4*. An *Oxford Cryosystems Cryostream* low-temperature device [38] was used for cooling the samples at 200 K. The structures were solved by direct methods using the SIR92 program [36]. The refinements were carried out by full-matrix least-squares

Table 5. *Selected Experimental Parameters in the Absolute Structure Determination of Compound* **III**

Crystal	A	B	C
Morphology	T1	T1	T2
No. of reflections/parameter	6.2	6.1	6.1
R/R_w	0.037/0.044	0.033/0.039	0.036/0.037
Abs. struct. parameter[a]) [37]:			
Coordinates of BNDA (*P*)-enantiomer	0.19(30)	0.16(27)	0.80(35)
Coordinates of BNDA (*M*)-enantiomer	0.81(30)	0.84(27)	0.21(35)

[a]) The same results are obtained when the starting values of the absolute structure parameter were 0.0, 0.5, or 1.0.

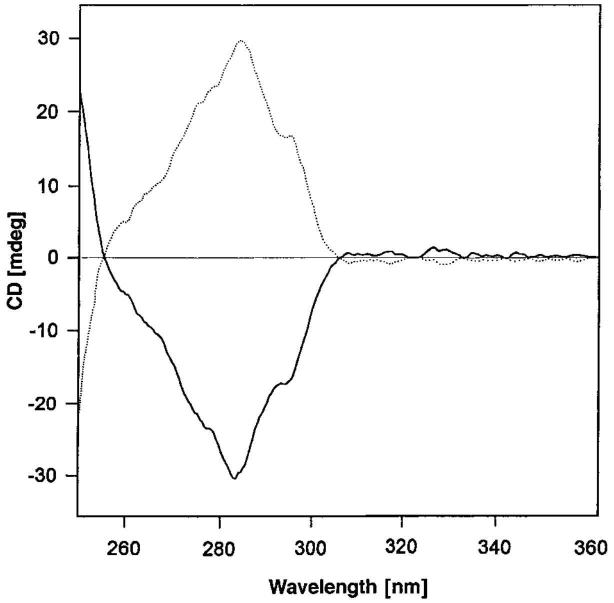

Fig. 6. *CD Spectra of salt* **III**. The A crystal of the salt studied by X-ray crystallography ((*P*)-configuration) corresponds to the continuous curve (negative *Cotton* effect).

procedures on F_o. The H-atoms, obtained from difference *Fourier* syntheses, were included as isotropic in the last cycles of refinement except in **III**, where all CH H-atom parameters have been kept fixed to increase the number of reflections per parameter ratio. Most of the calculations were performed using the XTAL3.2 system [39] and the PARST [40] program. In **III**, the *Friedel* pairs were collected and the absolute configuration determined according to the *Flack* refinement procedure [37] as implemented in the XTAL3.2 system [39]. The refinement of the *Flack* parameter was started at initial values of 0, 0.5, or 1 and in all cases converged to the same final value (*Table 4*). When the inverse structure is refined, the *Flack* parameter converges to 0.81(30), being again independent of the initial starting value. To assess a more reliable determination of the absolute configuration of **III**, two more crystals, B and C, were selected under the microscope and their absolute crystal structures refined; B displaying the same morphology as the previously solved one (type T1, A) and C showing enantiomorphic hemihedral faces (type T2). A summary of the most relevant experimental parameters for crystals, A, B, and C of compound **III** are gathered in *Table 5* for comparison purposes. The values of the *Flack* parameters among crystals are consistent in all cases, showing that crystals A and B are formed by the (*P*)-enantiomer [4] of the BNDA anion and crystal C by the (*M*)-enantiomer [4], and that both types of crystals are easily distinguishable by optical inspection. The weighting schemes were obtained (PESOS [41]) in an empirical way as to give no trends in $\langle w\Delta^2 F_o \rangle$ *vs.* $\langle F_o \rangle$ or $\langle \sin\theta/\lambda \rangle$. The atomic scattering factors were taken from the International Tables for X-Ray Crystallography, Vol. IV [42].

Crystallographic data (excluding structure factors) for the structures reported in this paper have been deposited with the *Cambridge Crystallographic Data Centre* as deposition No. CCDC-118849, CCDC-118848 and CCDC-118847 for **I**, **II** and **III** respectively. Copies of the data can be obtained, free of charge, on application to the CCDC, 12 Union Road, Cambridge CB21EZ, UK (fax: +44 (1223) 336033; e-mail: deposit@ccdc.cam.ac.uk).

Solution and Solid-State NMR. The high-resolution solid state ^{13}C-NMR spectra were obtained at r.t. on a *Bruker AC-200* spectrometer (UNED) working at 50.32 MHz under conditions of cross polarization (CP) and magic angle spinning (MAS) using a 7-mm *Bruker DAB 7* probehead that achieves rotation frequencies of *ca.* 3.5–4.5 kHz. Samples were carefully packed in ZrO_2 rotors (*ca.* 200 mg of material). The standard CPMAS pulse sequence was applied with a 7 μs ^{1}H-90° pulse width, 3–5 ms contact pulses, and 5 s repetition time, the spectral width being 20000 Hz. All chemical shifts are given with respect to the spectrometer reference frequency which was calibrated by the glycine signal at 176.1 ppm. Solution spectra (one and two-dimensions) were recorded on a *Bruker DRX-400* instrument. The samples prepared by mechanical co-grinding for solid-state NMR were prepared as follows: the mixture of 1:1 or 1:2 stoichiometric amounts of finely powdered samples of racemic BNDA and the corresponding pyrazole was carefully ground in a porcelain mortar and then introduced in the rotor.

Circular Dichroism and Polarimetry. Racemic BNDA absorbs at 265 and 339.5 nm in 95% EtOH. The CD spectra were recorded on a *Model J720* circular dichroism spectrophotometer (*Jasco*, Tokyo). To adjust the ellipticity (vertical axis) of *Fig. 6*, a pair of hemihedral crystals of similar size were selected and then, by dilution of the more concentrated, both curves were made similar. The microscope used for the triage was a *Nikon* (20 magnifications). The photographs of the crystals (*Fig. 5*) were taken with a *Zeiss* microscope, model *Temi SV 6* (8 to 50 magnifications). The specific rotations at 25° were determined with a *Perkin Elmer* model *241* polarimeter (sodium line, $\lambda_{\max} = 589$ nm) using *ca.* 1.2 mg of a crystal in 1.5 ml of EtOH. To a negative *Cotton* effect corresponds an $[\alpha]_D^{25} = -100 \pm 5$.

Note added on the proof. – Prof. *Carlo Rosini* (C. Rosini, R. Tanturli, P. Pertici, P. Salvadori, *Tetrahedron: Asymm.* **1996**, *7*, 2971) has drawn our attention to a seminal paper by *Mason et al.* (S. F. Mason, R. H. Seal, D. R. Roberts, *Tetrahedron* **1974**, *30*, 1671) where the CD spectrum of (−)-BNDA was reported and assigned to the (*S*)-configuration. This conclusion is consistent with our experimental determination ((−)-(*S*)-**1** or (−)-(*P*)-**1**).

REFERENCES

[1] L. Pasteur, *C. R. Acad. Sci.* **1848**, *26*, 535.

[2] L. Pasteur, *Ann. Chim. Phys.* 3ème Série, **1850**, *28*, 56.

[3] J. Jacques, A. Collet, S. H. Wilen, 'Enantiomers, Racemates, and Resolutions', Krieger Publishing Co., Malabar, Florida, 1994, p. 217.

[4] E. L. Eliel, S. H. Wilen, 'Stereochemistry of Organic Compounds', John Wiley & Sons, New York, 1994, p. 299, 1120.

[5] E. Weber, in 'Shape and Symmetry in the Design of New Hosts', in 'Comprehensive Supramolecular Chemistry', Eds. D. D. MacNicol, F. Toda, R. Bishop, Pergamon, Oxford, 1996, Vol. 6, p. 535.

[6] M. Czugler, J. G. Angyan, G. Naray-Szabo, E. Weber, *J. Am. Chem. Soc.* **1986**, *108*, 1275.

[7] T. Ohta, M. Ito, K. Inagaki, H. Takaya, *Tetrahedron Lett.* **1993**, *34*, 1615, and references therein.

[8] J. A. S. Smith, B. Wehrle, F. Aguilar-Parrilla, H. H. Limbach, C. Foces-Foces, F. H. Cano, J. Elguero, A. Baldy, M. Pierrot, M. M. T. Khursid, J. B. Larcombe-McDouall, *J. Am. Chem. Soc.* **1989**, *111*, 7304.

[9] F. Aguilar-Parrilla, O. Klein, J. Elguero, H. H. Limbach, *Ber. Bunsen-Ges. Phys. Chem.* **1997**, *101*, 889.

[10] L. Infantes, C. Foces-Foces, J. Elguero, *Acta Crystallogr., Sect. B* **1999**, *55*, 441.

[11] F. Toda, K. Tanaka, J. Elguero, Z. Stein, I. Goldberg, *Chem. Lett.* **1988**, 1061.

[12] F. Toda, K. Tanaka, C. Foces-Foces, A. L. Llamas-Saiz, H. H. Limbach, F. Aguilar-Parrilla, R. M. Claramunt, C. López, J. Elguero, *J. Chem. Soc., Chem. Commun.* **1993**, 1139.

[13] F. Toda, K. Tanaka, C. Foces-Foces, L. Infantes, R. M. Claramunt, C. López, J. Elguero, *J. Phys. Org. Chem.* **1996**, *9*, 611.

[14] F. H. Allen, J. E. Davies, J. J. Galloy, O. Johnson, O. Kennard, C. F. Macrae, E. M. Mitchell, J. F. Mitchell, J. M. Smith, D. G. Watson, *J. Chem. Info. Comput. Sci.* **1991**, *31*, 187.

[15] J. Bernstein, R. E. Davis, L. Shimoni, N.-L. Chang, *Angew. Chem., Int. Ed.* **1995**, *34*, 1555.

[16] L. Leiserowitz, *Acta Crystallogr., Sect. B* **1976**, *32*, 775. M. A. Neumann, S. Cracium, A. Corval, M. R. Johnson, A. J. Horsewill, V. A. Benderskii, H. P. Trommsdorff, *Ber. Bunsen-Ges. Phys. Chem*. **1998**, *102*, 325. T. Loerting, K. R. Liedl, *J. Am. Chem. Soc*. **1998**, *120*, 12595.
[17] F. H. Cano, M. Martínez-Ripoll, *J. Mol. Struct.* **1992**, *258*, 139.
[18] B. K. Vainshtein, V. M. Fridkin, V. L. Indenbom, 'Modern Crystallography II', Springer-Verlag, Berlin, Heidelberg, New York, 1982, p. 87.
[19] A. Baldy, J. Elguero, R. Faure, M. Pierrot, E. J. Vincent, *J. Am. Chem. Soc*. **1985**, *107*, 5290.
[20] J. Elguero, M. L. Jimeno, G. I. Yranzo, *Magn. Reson. Chem*. **1990**, *28*, 807.
[21] C. Foces-Foces, A. L. Llamas-Saiz, P. Lorente, N. S. Golubev, H. H. Limbach, *Acta Crystallogr., Sect. C* **1999**, *55*, 377.
[22] N. S. Golubev, G. S. Denisov, S. N. Smirnov, H. H. Limbach, *Z. Phys. Chem*. **1996**, *196*, 73.
[23] I. Alkorta, H. H. Limbach, P. Lorente, J. Elguero, unpublished results.
[24] A. C. Legon, C. A. Rego, *Chem. Phys. Lett*. **1989**, *157*, 243; **1989**, *162*, 468.
[25] M. Ramos, I. Alkorta, J. Elguero, N. S. Golubev, G. S. Denisov, H. Benedict, H. H. Limbach, *J. Phys. Chem. A* **1997**, *101*, 9791.
[26] H. Benedict, H. H. Limbach, M. Wehlan, W. P. Fehlhammer, N. S. Golubev, R. Janoschek, *J. Am. Chem. Soc*. **1998**, *120*, 2939.
[27] C. L. Perrin, J. B. Nielson, Y.-J. Kim. *Ber. Bunsen-Ges. Phys. Chem*. **1998**, *102*, 403.
[28] M. Caira, L. R. Nassimbeni, A. F. Wildervanck, *J. Chem. Soc., Perkin Trans. 2* **1995**, 2213.
[29] L. Szente, in 'Preparation of Cyclodextrin Complexes', in 'Comprehensive Supramolecular Chemistry', Eds. J. Szejtli, T. Osa, Pergamon, Oxford, 1996, Vol. 3, p. 243.
[30] J. Catalán, J. L. M. Abboud, J. Elguero, *Adv. Heterocycl. Chem*. **1987**, *41*, 187.
[31] R. Bishop, G. A. Downing, D. C. Craig, M. L. Scudder, *J. Inclusion Phenom*. **1998**, *31*, 145.
[32] E. Weber, I. Csöregh, B. Stenslund, M. Czugler, *J. Am. Chem. Soc*. **1984**, *106*, 3297; I. Csöregh, A. Sjögren, M. Czugler, M. Cserzö, E. Weber, *J. Chem. Soc., Perkin Trans. 2* **1986**, 507.
[33] D. E. Appleman, LSUCRE, Program for least-squares refinement of reticular constants. US Geological Survey, Washington DC, 1984.
[34] J. Hornstra, H. Vossers, *Philips Technical Rev*. **1973**, *33*, 61.
[35] W. H. Zachariasen, *Acta Crystallogr*. **1967**, *23*, 558.
[36] A. Altomare, M. C. Burla, M. Camalli, G. Cascarano, C. Giacovazzo, A. Guagliardi, G. Polidori, SIR92, *J. Appl. Crystallogr*. **1994**, *27*, 435.
[37] H. D. Flack, *Acta Crystallogr., Sect A* **1983**, *39*, 876.
[38] J. Cosier, A. M. Glazer, *J. Appl. Crystallogr*. **1986**, *19*, 105.
[39] S. R. Hall, H. D. Flack, J. M. Stewart, Xtal3.2, Eds. Univ. of Western Australia, Lamb, Perth, 1994.
[40] M. Nardelli, *Comput. Chem*. **1983**, *7*, 95.
[41] M. Martínez-Ripoll, F. H. Cano, Program not published, 1975.
[42] International Tables for X-Ray Crystallography, Kynoch Press, Birmingham, 1974, Vol. IV.

Received July 22, 1999